Autowave Model of the Transition from Stable Plastic Flow to Ductile Failure in Solids

L. B. Zuev

Institute of Strength Physics and Materials Science, SB RAS,

2/4, Akademicheskii Ave., Tomsk, 634021, Russia

lbz@ispms.tsc.ru

Keywords: plasticity, defects, failure, transition, autowaves

Abstract. Plastic flow evolution was investigated for various metals and alloys, which differed in chemical bond and crystal lattice type (BCC/FCC/HCP), structural state (single-crystal/polycrystalline) and deformation mechanisms (dislocation glide/twinning). On the base of conclusive evidence it is attempted to explain the phenomenon of plastic flow localization by invoking a fundamental principle of quantum mechanics.

Introduction

This paper was originated as a series of experimental study of plastic flow that was carried on for the recent two decades. The main findings of this study show that the plastic flow tends to localize at all the scale levels [1]. For a researcher in plasticity physics the macro-scale level is obviously the most convenient one since it serves to provide a unified explanation for a variety of plastic flow localization phenomena with striking regularities which are usually left unexplained. Thus it is found that (i) the plastic flow would exhibit a localization behavior from yield point to failure; (ii) each flow stage is characterized by the emergence of a specific localization pattern; (iii) the occurrence of localization patterns is explained as due to the generation of autowaves (self-excited waves); (iv) the latter waves are associated in turn with the processes of self-organization of defects.
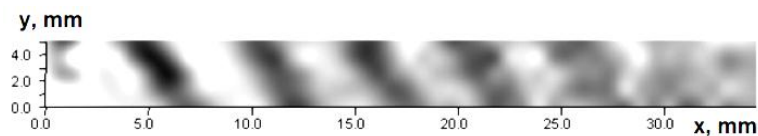

Fig. 1. Localization zones (dark bands) in the test sample

The kinematic observations were carried on with the aid of a specially developed technique related to speckle photography [1]. A typical example of autowave patterns occurring in the deforming medium is shown in figure 1. The propagation velocity, wavelength and frequency were defined experimentally for the autowaves in question. The values obtained differ fundamentally from those observed for elastic (ultrasound) waves [2] and plasticity waves [3], i.e. $10^{-5} < V_{aw} < 10^{-4}$ m·s^{-1} $<< V_{sound} \approx 3 \cdot 10^3$ m·s^{-1}; $\lambda \approx 10^{-2}$ m $>> b \approx 5 \cdot 10^{-10}$ m (here b is the Burgers vector of dislocations) and $10^{-3} < \omega < 10^{-2}$ Hz.

Dispersion relation for localized plastic flow autowaves: experimental results

The nature of autowave processes involved in plastic flow localization is conveniently addressed using the dispersion relation $\omega(k)$ derived for easy glide and linear work hardening stages [4], i.e.

$$\omega(k) = \omega_0 \pm \alpha(k - k_0)^2, \qquad (1)$$

where α, ω_0 and k_0 are constants which depend on the stage of work hardening and the kind of material (see figure 2). Note that for the stage of easy glide $\alpha < 0$ and for the stage of linear work hardening $\alpha > 0$.

As is seen from figure 3, equation (1) can be brought to canonical form by the substitution of $\omega = \omega_0 \cdot \tilde{\omega}$ and $k = k_0 + \tilde{k} \cdot (\text{sign}\,\alpha \cdot \alpha / \omega_0)^{-1/2}$ to give $\tilde{\omega} = 1 \pm \tilde{k}^2$ (here $\tilde{\omega}$ is the dimensionless frequency; $\tilde{k}$ is the dimensionless wave number and $\text{sign}\,\alpha$ is a signum function of the coefficient α). Thus we obtain the appropriate dispersion relation of quadratic form, which satisfies the Schrödinger nonlinear equation [5] and is descriptive of self-organization processes in nonlinear media. This is a formal proof of the fact that self-organization and plastic flow localization are closely involved processes.

A correspondence between the localized plastic flow autowave and the effective mass

The effective mass is conventionally found[6] from the dispersion law $\omega(k)$ as

$$m_{aw} = \hbar \left(d^2 \omega / dk^2 \right)^{-1}, \qquad\qquad (2)$$

where $\hbar = h/2\pi$ is the Planck constant. The effective masses obtained for single γ-Fe crystals and polycrystalline Al are $m_{aw}^{(Fe)} = 0.6$ amu and $m_{aw}^{(Al)} = 0.1$ amu, respectively. Note that effective masses of the same magnitude can be calculated from the de Broglie equation [6] as

$$m_{aw} = h / \lambda V_{aw}. \qquad\qquad (3)$$

Similar calculations were performed by addressing autowaves in [7]. To test the validity of this idea, m_{aw} values were calculated from (3), using the autowave characteristics obtained for a number of metals and alloys [1]; the results obtained are listed in the table. Apparently, the calculated values have about the same scale magnitude, i.e. $m_e \ll m_{aw} \approx 1$ amu (here m_e is the rest mass of electron; 1 amu = $1.67 \cdot 10^{-27}$ kg is atomic mass unit). The average mass calculated from (3) for the same metals is $\langle m_{aw} \rangle = (2.2 \pm 0.3) \cdot 10^{-27}$ kg = 1.32 ± 0.2 amu.
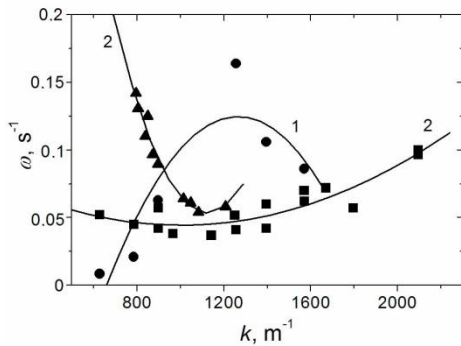

Fig. 2. Dispersion relation $\omega(k)$ for easy glide (1) and linear work hardening stages (2): single-crystal Cu, Sn and Fe (●); single γ-Fe crystal (■); polycrystalline Al (▲)
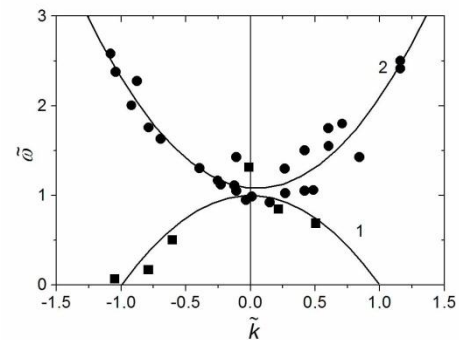
Fig. 3. A generalized relation $\tilde{\omega}(\tilde{k})$ for easy glide (1) and linear work hardening stages (2): single γ-Fe crystal and polycrystalline Al

Then the volume was calculated as $\Omega = m_{aw}/\rho$ (here m_{aw} is the effective mass and ρ is metal density); hence the effective size $d_\Omega = \Omega^{1/3}$. The ratios d_Ω / r_{ion} listed in the Table suggest that the volumes and ion radii calculated for the studied metals [8] are close in magnitude.

The average $\langle d_\Omega / r_{ion} \rangle$ obtained for all the studied materials is 0.51±0.1. Normalization of the values m_{aw} was performed in atomic mass units, M_{at}. Then the dimensionless mass was introduced, i.e. $s = m_{aw}/M_{at} << 1$. As is seen from figure 4, the value s grows linearly [9] with increasing electron concentration n as

$$s = s_0 + \kappa \cdot n = 1.6 \cdot 10^{-2} + 0.17 \cdot 10^{-2} \cdot n . \tag{4}$$

The latter dependence is determined by the viscous drag of dislocations due to the occurrence of phonon and electron gases in metals [1].

A question I would like to address at this point is whether it is possible to propose that a certain quasi-particle exists which corresponds to the localized plastic flow autowave generated in the deforming solid. Using equation (3), the mass and the effective size of the quasi-particle can be calculated from the data listed in the table. The values obtained are $0.5 \leq m_{aw} \leq 2$ amu and $d_\Omega \approx r_{ion}$. The use of this approach which has received wide application in the physics of solids [10], enables one to unambiguously relate the characteristics of the deformation macrolocalization process to those of the crystal lattice.

Table. Microscopic characteristics calculated from the data on localized plastic flow autowaves

| Metal	$\lambda \cdot 10^3$ [m]	$V_{aw} \cdot 10^5$ [m/s]	m_{aw} [amu]	$s \cdot 10^2$	$\rho \cdot 10^{-3}$ [kg/m^3]	$\Omega \cdot 10^{27}$ [m^3]	$d_\Omega \cdot 10^9$ [m]	$r_{ion} \cdot 10^9$ [m]	$\dfrac{d_\Omega}{r_{ion}}$
	4.5	8.0	1.1	1.74	8.9	0.21	0.059	0.128	0.46
Zn	4.9	7.6	1.07	1.66	7.1	0.25	0.063	0.071	0.89
Al	7.2	11	0.50	1.87	2.7	0.31	0.068	0.143	0.48
Zr	5.5	3.5	2.05	2.24	6.5	0.53	0.081	0.16	0.50
Ti	7.0	5.0	1.1	2.3	4.5	4.2	0.075	0.146	0.51
V	4.0	7.0	1.42	2.81	6.1	0.33	0.069	0.135	0.51
Nb	4.5	4.0	2.21	2.5	8.6	0.41	0.074	0.069	1.08
γ-Fe	5.0	5.1	1.76	2.81	7.9	0.33	0.069	0.127	0.54
α-Fe	4.3	5.2	1.77	3.0	7.9	3.75	0.072	0.127	0.57
Ni	3.5	6.0	0.89	3.24	8.9	0.32	0.068	0.125	0.54
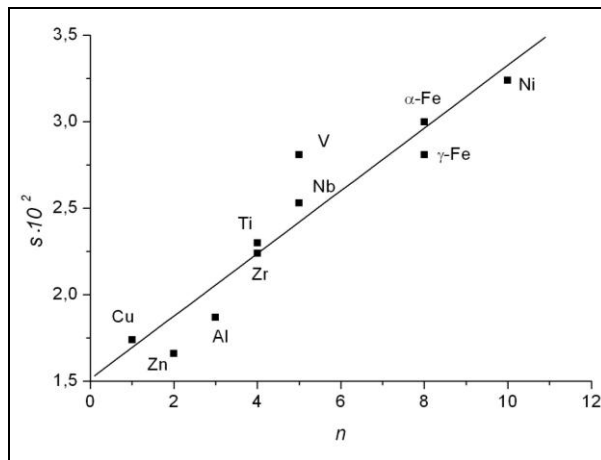
Fig. 4. Dimensionless mass s as a function of electron concentration n;
correlation coefficient ~0.95

A two-component model of plastic flow

I would like to single out the physical aspect of the problem considered herein. This consists in the fact that a unified account is sought for two closely interrelated categories of events. Indeed, an elementary plasticity act (shear) is capable of generating an acoustic pulse, which in turn would initiate a new shear. Thus one has to account for the causal relationship between the two kinds of events occurring simultaneously in the deforming medium, i.e. the dislocation shears, which initiate the relaxation of stresses, and the acoustic emission pulses, which are responsible for the redistribution of stresses. Taking this approach, the idea of spontaneous layering[1] as applied to a system undergoing self-organization was formulated. Spontaneous layering would cause formation of two interrelated subsystems, an informative and a dynamic one. For the case of deforming medium, the choice of appropriate subsystems appears to be sufficiently simple. Thus the role of information signals, which cause relaxation of shears, is assigned to acoustic emission pulses (phonons) generated by other, similar shears. The resultant redistribution of the elastic field would initiate new shears in the dynamic dislocation subsystem.

The spatial scales of macro- and microscopic quantities under discussion differ crucially in the range $10^6 < \lambda/r_{ion} < 10^7$. Nonetheless, it is established that the product of two macro-characteristics of autowave processes, i.e. $\lambda \cdot V_{aw}$, and the product of two micro-characteristics of the respective metal, i.e. $r_{ion} \cdot V_{\perp}$, are related linearly as

$$\lambda \cdot V_{aw} \approx \zeta_{Me} \cdot r_{ion} \cdot V_{\perp} , \qquad (5)$$

where $V_{\perp}$ is the rate of transverse elastic waves [11]. The numerical factor differs in the range $0.52 \leq \zeta_{Me} \leq 0.82$ for various metals, with the average being $\langle \zeta \rangle \approx 0.62$. The physical meaning of the latter factor might be deduced from equation (5) represented as

$$m_{aw} = h/\lambda V_{aw} \approx \zeta_{Me}^{-1} \cdot h/r_{ion}V_{\perp} , \qquad (6)$$

where $h/r_{ion}V_{\perp} \equiv m_{ph}$ is the phonon mass. From equation (6) follows that $m_{aw} \approx 1.6 m_{ph}$, i.e.

$$1.5 m_{ph} \leq m_{aw} \leq 2 m_{ph} . \qquad (7)$$

The latter equation corresponds to the mechanism of dislocation generation due to phonon condensation [12]. Thus, a significant role in the evolution of localized plastic flow autowaves is assigned to the lattice characteristics.

The above should not be regarded as a mere formalization of the relationship between the characteristics of plastic flow localization on the one hand and the acoustic characteristics of the deforming medium on the other. A particular emphasis is placed herein on the role of the phonon subsystem in the evolution of localized plastic deformation, which involves (i) relaxation acts due to the motion of dislocations, dislocation ensembles and localized plastic flow autowaves and (ii) generation of elastic waves due to the acoustic emission, i.e. redistribution of elastic strains involving large-scale and small-scale relaxation events.

Generally, the above phenomena are studied independently. However, these might be grouped together in accordance with the concept [13] to address a system undergoing self-organization, which separates into two related subsystems, i.e. an informative and a dynamic one. Acoustic emission signals serve as deformation carriers for the deforming system. These are generated by relaxation shears, which initiates redistribution of elastic strain fields to cause new shears in the dynamic subsystem of mobile defects.

Apparently, relation (6) serves to formalize the connection between the kinetic characteristics of the above subsystems, i.e. the propagation velocity of elastic waves and the motion rate of dislocations in the vicinity of stress concentrators, respectively. In the frame of the proposed

model, acoustic emission pulses would control the development of localized plastic flow, while those having sufficiently high energy would activate new plasticity events [14].

Important features of two component model
The nature of self-organization occurring in complex media is being simulated by various models that have one basic assumption in common [14]. Built into these models is the notion that complex open systems capable of self-organization tend to separate spontaneously into an information (control) subsystem and a dynamic one. This notion can be extended to take account of deforming media. In this instance, it may be reasonably assumed that acoustic emission signals that are emitted during elementary relaxation acts of plastic flow would play the role of an information subsystem and the processes of motion of dislocations or dislocation ensembles that are responsible for material form changing would represent a dynamic subsystem. In the framework of the given approach, the process of plastic flow would be associated with interrelated concerted events occurring in the defect and phonon subsystems of the deforming crystal (see fig. 5). Thus, the proposed two component model differs radically from various dislocation models that have been put forward to account for the evolution of defect subsystem alone. The evolution of plastic flow in each localized deformation nucleus correlates closely with the other nuclei although they are separated from one another at a macroscopic distance of the order of λ (autowave length). In order to attribute for the latter fact, it should be born in mind that acoustic emission impulses play an important role in plastic deformation, taking into account, in particular, their great path length.
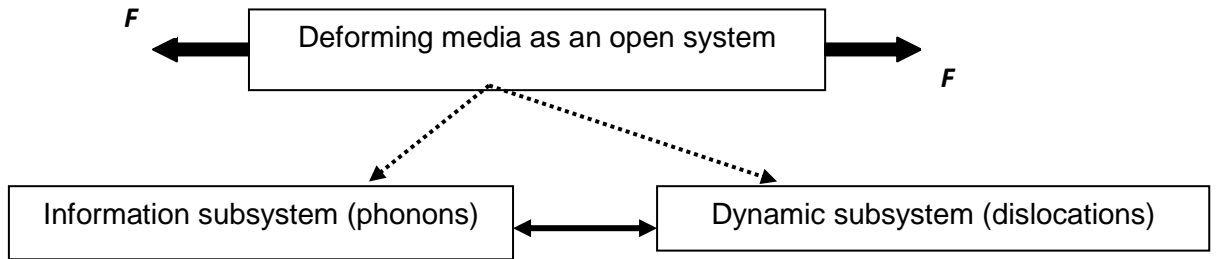

Fig. 5. Scheme of principle for two component model of plasticity

The above approach is consistent with the two-component plastic flow model proposed in [1] in which equations of reaction-diffusion type are used to describe the autocatalytic and the damping factor, i.e. plastic deformation ε and elastic stresses σ, respectively. The rates of variation of deformations and stresses are given above as $\dot{\varepsilon} = f(\varepsilon,\sigma) + D_{\varepsilon}\varepsilon''$ and $\dot{\sigma} = g(\sigma,\varepsilon) + D_{\sigma}\sigma''$, respectively. The nonlinear functions $f(\varepsilon,\sigma)$ and $g(\sigma,\varepsilon)$ have the meaning of local rates of variation of deformations and stresses, respectively, and the "diffusion addends" $D_{\varepsilon}\varepsilon''$ and $D_{\sigma}\sigma''$ are responsible for the macro-scale re-distribution of deformations and stresses.

In the context of the proposed model, these equations are taken to describe variations occurring, respectively, in the dynamic and information subsystems that differ in scale. The subsystems' scales enter into the diffusion coefficients that are represented in a general form as $D \approx V \cdot L$. For the information subsystem, the quantity $L \approx \lambda$ is of the order of specimen length; for the dynamic subsystem, this is close to the size of a dislocation ensemble, i.e. $L \approx \bar{d} << \lambda \, \square.$ The numerical $\lambda/\bar{d}$ ratio can be accounted for by comparing the transport coefficients from equations above for deformations and stresses.

Thus, the two component model being developed is based on the assumption that the following well-known effects are closely interrelated, i.e.

- deformation proper that is caused by the motion of lattice defects, in particular, dislocations, i.e. the dynamic subsystem;
- acoustic emission that accompanies the action of any plastic flow mechanisms, i.e. the information subsystem.

Autowave generation at stress concentrators

As discussed above, the localized plastic flow waves would be generated in all deforming materials. Therefore, it needs to be ascertained what gives rise to the waves in question. It is believed that the wave generation is due to the stress concentrators which play an important role in the plastic flow evolution [1]. On this assumption a series of experiments was conducted to elucidate the cause-and–effect relationship between the localized plastic flow waves and the macroscopic stress concentrators occurring in the deforming solid.

Accurately modeling a macroscopic concentrator of stresses involves growing a fatigue crack in a plastically deforming material. These simulations were conducted in order to establish the regularities exhibited by plastic flow dynamics by viscous fracture. To this end, an *in situ* investigation of the deforming specimen was carried on to trace the changes in the plastic deformation zone located at the tip of a developing crack. The geometry of test specimens and the loading conditions differ significantly from those described in the monograph [1]; therefore, the procedure used should be described in some detail. The test specimens having dimensions 90×20×10 mm were cut out from a 0.2 mm sheet of low carbon steel (0.08 % C). In the middle of the test specimen was an 8-mm V-notch, which had curvature (Ø 0.2 mm) at its tip where a 2-mm fatigue crack was to be grown. The three-point loading was conducted on a universal testing machine 'Instron-1185', with the separation between the loading device supports being 80 mm and the crosshead motion rate, 0.5 mm/min.

For the specimen under loading, *in situ* recording of displacement vector fields was conducted on an 'ALMEC' unit, using the method of double exposure speckle photography. The registration was carried on step by step, with each step corresponding to a 100-μm displacement of the movable support. The displacement vector fields were recorded for individual points on the specimen surface from the beginning of loading to specimen fracture to an accuracy of ~1 μm. Special software was designed for speckle photograph decoding, which enables one to obtain data files storing displacement vectors U and point co-ordinates. The vector U is preset with the respective modulus U and the angle α the vector makes with the specimen axis x. The location of the crack's tip $O(x_0, y_0)$ is pre-assigned in the same co-ordinates.

In the context of linear fracture mechanics, the displacement vector field at the crack's tip is determined in the polar co-ordinates r and φ chosen on the strength of problem symmetry and is given by the following expression of the form

$$U = \frac{K_1\sqrt{r}}{Gk^{\bullet}}[(2k+1)^2\cos^2\frac{\varphi}{2} + 2(4k^2-1)\cos\frac{\varphi}{2}\cos\frac{3\varphi}{2} + (2k-1)^2\sin^2\frac{\varphi}{2} +$$

$$+ 2(2k-1)^2\sin\frac{\varphi}{2}\sin\frac{3\varphi}{2} + (2k-1)^2]^{\frac{1}{2}}, \qquad (8)$$

where r is the distance counted over the ray from the crack tip O; φ is the angle between the direction of the ray r and the direction of crack propagation y; G is the shear modulus; K_1 is the stress intensity coefficient; k is the constant determined by the Poisson ration of material and by the kind of stressed state. It follows from expression (6.17) that for elastically deformed material zone, $U \sim r^{1/2}$. On the border between the elastically and plastically deformed material volumes the latter regularity would apparently break down, which enables detection of such a border, using the following procedure.

The displacement vector U is first measured at a step of 3º for the angle φ over 60 rays r_i to give a total of 100 U values; then the distance from the crack tip r^* is determined. The experimental dependences $U(r^{1/2})$ obtained for the latter sections of the rays r_i are interpolated by the least-squares method to give, in accordance with (8), linear dependencies. The correlation coefficient obtained for these dependencies serves as a criterion of linearity. The current U values are eliminated successively on going from the crack tip r^* over each r_i ray to give a maximal constant value of the correlation coefficient. As a result, a set of boundary distances is obtained such that in the region $r > r^*$ the regularities of linear fracture mechanics would hold good, with the geometry of r^* arrangement defining the boundary between the elastically and plastically deforming specimen zones.

With growing total deformation, the plasticity zone is found to change gradually. At first the zone would mainly evolve in the direction y in which the original crack propagates. Before the onset of yielding, it is anomalously elongated in the direction $\varphi = 20\ ...25º$. The advance of the plastic zone border might be likened to the Lüders band propagation, which is observed for the yield plateau in materials whose flow curve shows a sharp yield point. Plastic zones generally have broken borders, which is probably due to the spatial inhomogeneity of plastic flow. The above suggests, however, that plastic deformation would also exhibit a temporal inhomogeneity. Thus local shear macro-bands occurring in certain areas of the deforming specimen might disappear to emerge and develop in other regions. Therefore, in the entire half-space in front of the crack tip no steady growth of the plasticity zone is observed; instead portions of its border would advance in a jump-wise way. Thus the emergence of the above pattern is due to a more complicated stressed state of material at the crack tip relative to that observed by the Lüders band propagation in tensile specimens.

Of great significance is the data on material behavior in a plasticity zone located in the vicinity of stress concentrator where the relationships of linear fracture mechanics would not hold good and the material would deform plastically. Strong evidence for the behavior of material under loading in the above zone has been provided by the analysis of plastic tensor component fields for a planar case

$$\varepsilon_{ij} = \begin{vmatrix} \varepsilon_{rr} & \varepsilon_{r\varphi} \\ \varepsilon_{\varphi r} & \varepsilon_{\varphi\varphi} \end{vmatrix}. \tag{9}$$

All the plastic distortion tensor components, i.e. $\varepsilon_{rr} = \partial U_r/\partial r$, $\varepsilon_{\varphi\varphi} = 1/r(\partial U_{\varphi\varphi}/\partial\varphi) + U_r/r$, $\varepsilon_{r\varphi} = \varepsilon_{\varphi r} = 1/2[1/r(\partial U_r/\partial\varphi) + \partial U_\varphi/\partial r - U_\varphi/\partial r]$, can be derived from the experimental data array $U(x, y)$, using numerical differentiation of displacement vector ε_{ij} values from the polar co-ordinates r and φ obtained for each individual point on the specimen surface where the vector U is determined for loading time increments.

Figure 6 illustrates the spatial distributions of plastic distortion tensor components against loading time. Evidently, an ordered space-periodic system of localized deformation nuclei emerges in the plasticity zone, with the separation between the maxima being ~2...3 mm. The above pattern can be regarded as an early stage of the generation of localized plastic flow wave. With increasing total deformation, the shape of generated waves would change, which might be attributed to the inhomogeneity of displacement field caused by the stress concentrator (crack).

Summary
When considered in the context of the proposed model, the interaction between localized deformation nuclei is attributed to the exchange interaction by phonons. In this scenario it appears reasonable to assume that to the autowave of localized deformation corresponds a quasi-particle whose characteristics are determined by the autowave characteristics.

Further development of the proposed concept would enable one to group the localized plastic flow together with such phenomena as superfluidity and superconductivity, which are taken to be macro-scale manifestations of the deforming medium's quantum properties.
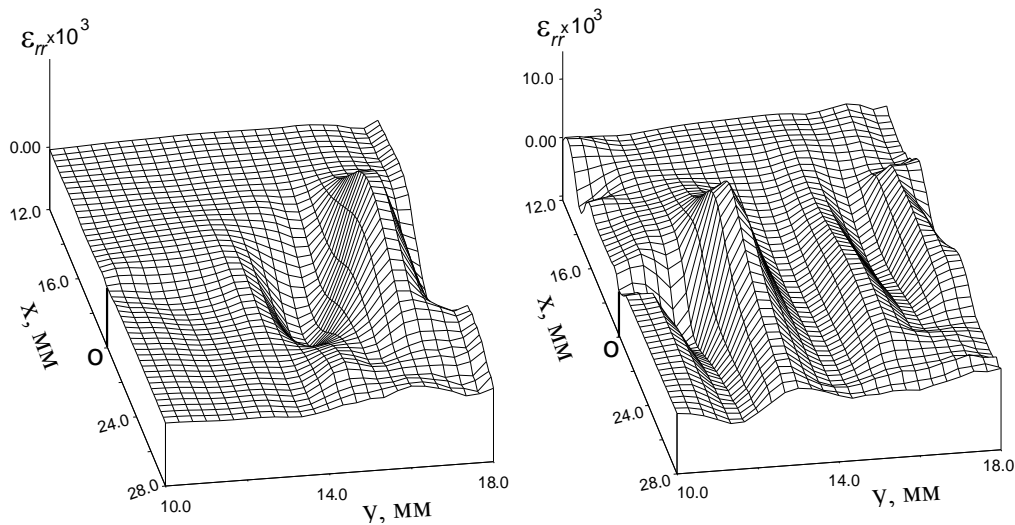

Fig. 6. A picture of autowave process generation in the vicinity of stress concentrator O

References
[1]   L.B. Zuev, V.I. Danilov and S.A. Barannikova: *Plastic Flow Macrolocalization Physics* (Nauka Publishers, Novosibirsk, 2008) (in Russian).
[2]   R.E. Newnham: *Properties of Materials* (University Press, Oxford, 2005).
[3]   *Basic Engeneering Plasticity*. Ed. D. Rees. (Buttreworth Heineman, London, 2006).
[4]   L.B. Zuev and S.A. Barannikova: Nat. Sci. Vol. 2, (2010), p. 476.
[5]   A. Scott: *Nonlinear Science* (University Press, Oxford, 2003) .
[6]   L.D. Landau and E.M. Lifshits: *Quantum Mechanics* (Pergamon Press, London, 1977).
[7]   L.B. Zuev: Ann. Phys. Vol. 16, (2007), p. 286.
[8]   W.B. Pearson: *The Crystal Chemistry and Physics of Metals and Alloys* (Wiley, New York, 1972).
[9]   L.B. Zuev: Int. J. Sol. Structures. Vol. 42, (2005), p. 943.
[10] J. M. Ziman: *Electrons and Phonons* (University Press, Oxford, 2001).
[11] A. Everest and K. Pohleman: *Master Handbook of Acoustic* (mcGraw-Hill, New York, 2009).
[12] H. Umezawa and H. Matsumoto: *Thermo Field Dynamics and Condensed States* (North-Holland Publ. Comp. Amsterdam, 1982).
[13] B.B. Kadomtsev: Physics-Uspekhi. Vol. 165, (1995), p. 967.
[14] L.B. Zuev and S.A. Barannikova: J. Mod. Phys. Vol. 1, (2010), p. 3.